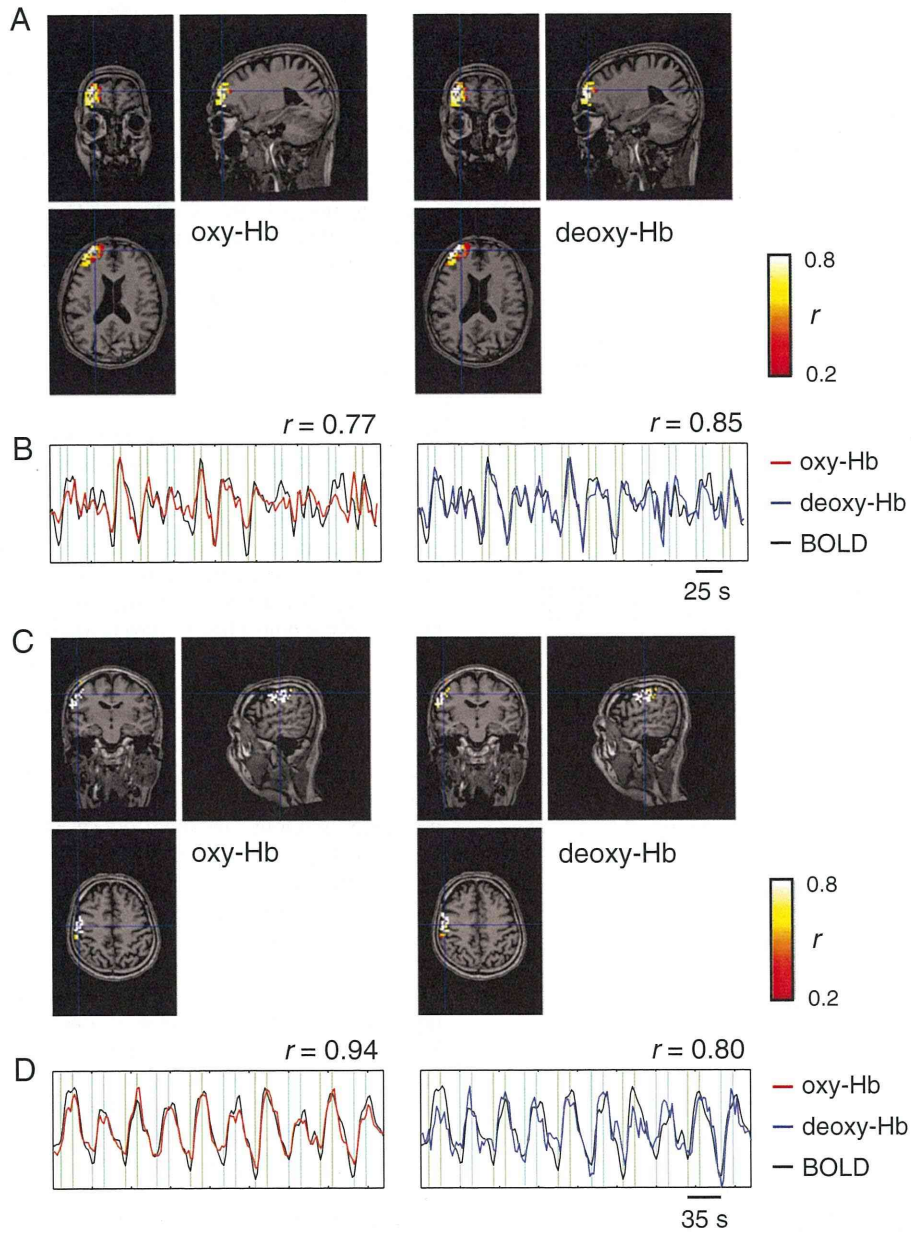

Fig. 5. Examples of correlation between NIRS-Hb signals and BOLD signals. (A) Example for WM task. Significantly correlated voxels ($p < 0.05$, FDR corrected for total number of object voxels) were superimposed on T1-weighted image. Sign of correlation coefficients for NIRS deoxy-Hb signals was inverted for comparison with result for NIRS oxy-Hb signals. (B) Time courses of NIRS oxy-Hb (red line) and NIRS deoxy-Hb signals (blue line) along with that for L-BOLD signal in GM (black), which corresponds to example (A). Sign of NIRS deoxy-Hb signal was inverted for comparison with L-BOLD signal. NIRS-Hb and L-BOLD signals were normalized to have the same range of amplitude and are shown in arbitrary units. (C) and (D) Example for TAP task, which is shown in the same manner as in (A) and (B).

the eyebrows) was used here. The results for LDF channel 2 were basically the same, as shown in the Supplementary Materials (Fig. S1). A one-sample *t*-test against zero indicated significant correlation coefficients only for the oxy-Hb signals for the WM task ($t(18) = 5.4$, $p < 5 \times 10^{-3}$). To investigate the dominance of the L-BOLD (GM) signals compared to the LDF signals for contribution to the oxy-Hb signals, we conducted a two-way ANOVA between signal type (L-BOLD (GM)/LDF) and task type (WM/TAP) for the correlation *Z*-values. The results revealed a significant main effect of signal type ($F(1, 66) = 13.6$, $p < 5 \times 10^{-4}$) with no main effect of task ($p = 0.91$) and no interaction ($p = 0.45$), indicating that the correlation between the NIRS oxy-Hb and L-BOLD (GM) signals was higher than that between the NIRS oxy-Hb and LDF signals.

Table 2
Basic results of voxel-based BOLD analysis for channel of interest.

	Gray matter		Soft tissue	
	WM	TAP	WM	TAP
Number of total voxels	266 ± 65	229 ± 89	235 ± 80	336 ± 107
Number of voxels correlated with oxy-Hb signals ± SD (Percentage ± SD)	162 ± 102 (58 ± 32%)	118 ± 86 (58 ± 41%)	12 ± 14 (6 ± 8%)	17 ± 18 (6 ± 8%)
Number of voxels correlated with deoxy-Hb signals ± SD (Percentage ± SD)	119 ± 117 (45 ± 42%)	128 ± 97 (66 ± 35%)	7 ± 9 (4 ± 6%)	13 ± 20 (6 ± 10%)

Correlation of NIRS-Hb signals with L-BOLD and LDF signals in block-averaged data

To further examine the relationship between the NIRS-Hb and L-BOLD (GM) signals, we calculated the time-locked block-averaged

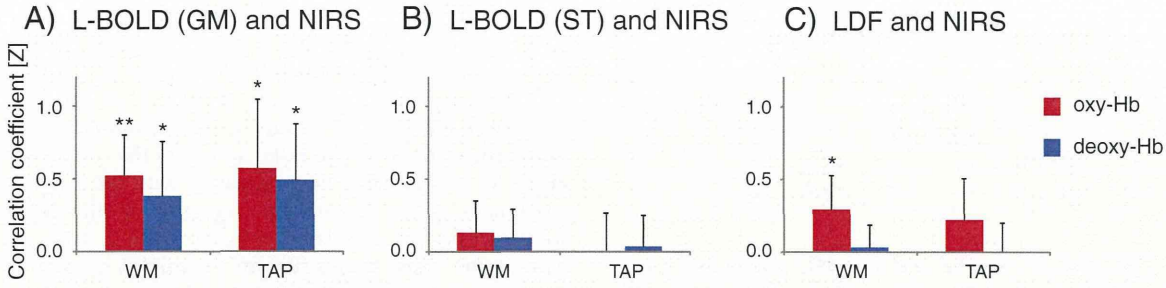

Fig. 6. Mean and standard deviation of correlation coefficients (*Z*-values from Fisher's transformation) for NIRS-Hb signals in activation area for WM task (n = 19) and TAP task (n = 16). (A) Correlation of L-BOLD signals in GM region with NIRS-Hb signals. (B) Correlation of L-BOLD signals in ST region with NIRS-Hb signals. (C) Correlation of LDF signals with NIRS-Hb signals. Sign of correlation coefficients for NIRS deoxy-Hb signals was inverted for comparison with results for oxy-Hb signals. Statistical significance against zero is shown ($^{**}p < 5 \times 10^{-6}$, $^{*}p < 5 \times 10^{-3}$). Bonferroni correction was applied for multiple comparisons.

timecourses as they represent purer task-related responses for each participant. The mean and standard error of the block-averaged timecourses across participants are shown not only for the NIRS-Hb and L-BOLD (GM) signals but also for L-BOLD (ST) and LDF signals (Fig. 7). In addition, the task-related signal changes were quantified by the effect size (Table 3). For both tasks, the NIRS oxy-Hb signals clearly increased along with an increase in the L-BOLD (GM) signals and a decrease in the NIRS deoxy-Hb signals. On the other hand, the L-BOLD (ST) signals tended to increase for the WM task and to decrease for the TAP task. In addition, the LDF signals for the WM task showed a clear increase for the WM task. The correlation coefficients for the block-averaged timecourses in different modalities, which are listed in Table 4, showed a tendency similar to the results shown by the continuous data (Fig. 6) as expected. In short, the L-BOLD (GM) signals showed a high correlation with the NIRS-Hb signals (mean $|r| > 0.5$) while the L-BOLD (ST) signals did not show such a tendency (mean $|r| < 0.22$). In addition, the LDF signals showed a high correlation with only the NIRS oxy-Hb signal for the WM task (mean $r = 0.52 \pm 0.46$) (Table 4).

Using the block-averaged timecourses, we compared the amplitudes of the task-related responses between the NIRS-Hb and L-BOLD (GM) signals (Fig. 8). For both tasks, the two signals showed significant correlation ($p < 0.05$), which means the participants with a stronger response in the NIRS-Hb signal also showed a stronger response in the L-BOLD (GM) signal in the fMRI data. Note that these block-averaged results were not due to a biased selection of participants, as shown by the supplementary result using all participants' data (Supplementary Materials, Fig. S2).

To identify other possible factors affecting the response amplitudes, we checked the scalp-cortex distance (SCD) for the COI. The means and SDs were 13.6 ± 2.2 and 17.6 ± 2.6 mm for the WM and TAP tasks, respectively. The SCD for the TAP task (sensorimotor area) was

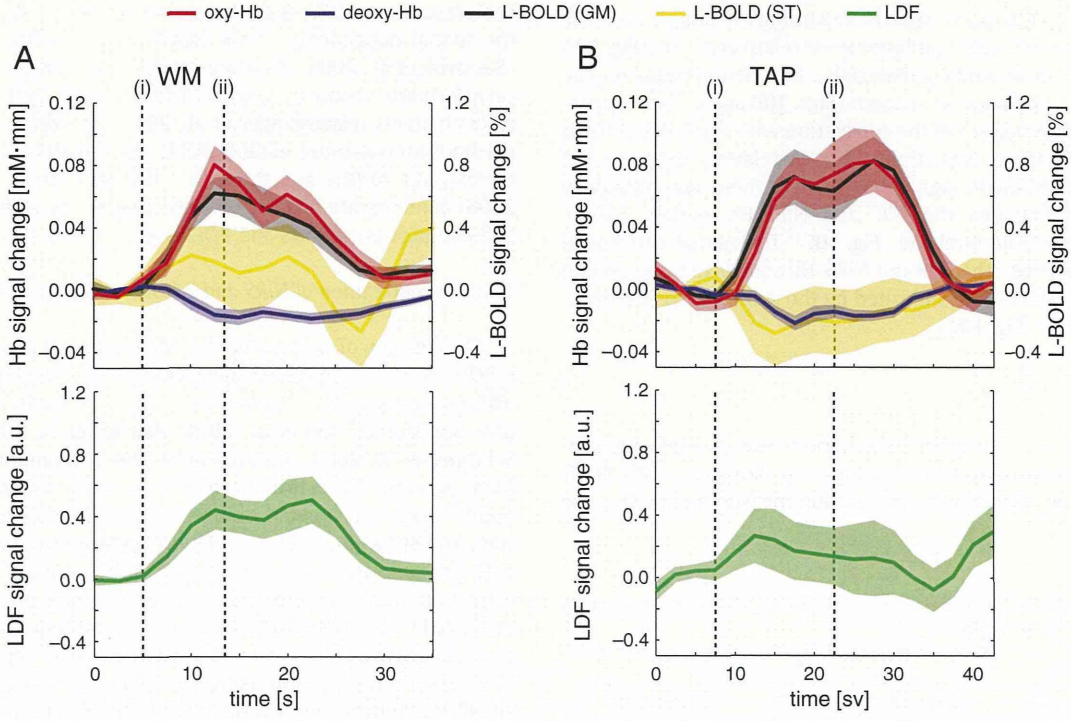

Fig. 7. Block-averaged timecourses of NIRS-Hb, L-BOLD, and LDF signals with standard error (transparent color region) for COI. LDF signals are average of data from two channels. (A) Time courses for WM task (N = 19). (i) Time of Target stimuli (start of encoding), (ii) Time of Test stimuli (end of maintenance and start of retrieval). (B) Time courses for TAP task (N = 16). (i) Time of task start (start cue presented), (ii) Time of task end (end cue presented).

Table 3
Mean ± standard deviation of effect size (d) of NIRS and BOLD signals in COI and LDF signals.

	NIRS		fMRI		LDF
	Oxy-Hb	Deoxy_Hb	L-BOLD (GM)	L-BOLD (ST)	
WM	2.56 ± 1.68	−1.62 ± 1.59	1.83 ± 1.23	0.29 ± 0.96	1.06 ± 1.48
TAP	3.22 ± 3.85	−2.01 ± 2.24	3.65 ± 5.57	−0.26 ± 1.28	0.76 ± 1.52

significantly larger than that for the WM one (PFC) (two-tailed t-test, $p < 5 \times 10^{-5}$). The means and SDs of the SCD for all NIRS channels are listed in the Supplementary Materials (Table S2).

Spatial distribution of temporal correlations of NIRS-Hb signals with L-BOLD and LDF signals

As an additional analysis, we examined the general tendency of the correlation coefficients between the NIRS and L-BOLD (GM) signals for a wide area using the data of Probe-1. The correlation coefficients between the NIRS-Hb and L-BOLD (GM) signals for all NIRS channels are mapped in Fig. 9A and show the spatial distribution. The middle to lower parts of the central area and upper parts of the bilateral ends indicate relatively high correlation coefficients for both tasks. The area dependency of the correlation pattern was examined by grouping the 52 NIRS channels into three areas on the basis of the results of clustering analysis (Fig. 9B). In Area 1 which mainly included BAs 2, 3, 10, 22, 40, and 46, the correlation coefficients between the NIRS-Hb and L-BOLD (GM) signals were significantly different from zero for both tasks. This is in agreement with the results for the activation area (COI). Fifteen NIRS channels adjacent to Area 1 were grouped as Area 2. Although the results for these channels showed a tendency similar to those for the channels in Area 1, the correlation coefficients were lower and statistically significant only for the oxy-Hb signals. In contrast to the results for the NIRS channels in Areas 1 and 2, the results for those in Area 3 (i.e., the ones around the center of the top lines of the NIRS probe holder and the bilateral temple area) showed almost no correlation between the NIRS-Hb and L-BOLD (GM) signals. Regarding the temple area, the distances between the scalp and brain were relatively large (Fig. 10A and Table S1 in Supplementary Materials). Correlation maps for the L-BOLD (ST) and LDF signals are shown (Figs. 10B and C) for comparison with the spatial pattern of the correlation with the L-BOLD (GM) signals. Although there was almost no correlation between the L-BOLD (ST) and NIRS-Hb signals (Fig. 10B), there was relatively large correlation between the LDF and NIRS-Hb signals, mainly around the center of the forehead (Fig. 10C). The spatial patterns of the correlation between the LDF and NIRS-Hb signals did not depend on the position of the LDF, as indicated by the similar maps for channel 1 and channel 2 (Fig. 10C).

Discussion

The present study examined the criterion-related validity of prefrontal NIRS-Hb signals by investigating their similarity with BOLD signals, the gold standard for brain-function measurements. Our use of a relatively reliable task paradigm to measure PFC activation in a large number of participants (N = 27) for simultaneous NIRS, fMRI, and LDF measurements enabled us to partially clarify the nature of the prefrontal NIRS-Hb signals. Statistical analysis demonstrated that prefrontal NIRS-Hb signals in the activation area were significantly correlated with the BOLD signals in the GM rather than those in the ST or skin blood flow measured with the LDF. Moreover, the amplitudes of the task-related responses of the NIRS-Hb signals were significantly correlated with the L-BOLD (GM) signals across participants. These results support the validity of using NIRS to measure hemodynamic signals originating from prefrontal cortical activation; i.e., it is comparable to using BOLD signals measured by fMRI.

Table 4
Mean ± standard deviation of correlation coefficient (r) across participants for block-averaged timecourses in COI.

	WM		TAP	
	Oxy-Hb	Deoxy-Hb	Oxy-Hb	Deoxy-Hb
L-BOLD (GM)	0.69 ± 0.26	−0.50 ± 0.35	0.60 ± 0.33	−0.56 ± 0.33
L-BOLD (ST)	0.22 ± 0.46	−0.04 ± 0.47	−0.14 ± 0.50	0.08 ± 0.48
LDF	0.52 ± 0.46	−0.17 ± 0.39	0.19 ± 0.37	0.01 ± 0.41

Voxel sphere for correlation analysis

To compare the BOLD signals with the NIRS-Hb signals, we first defined a voxel cluster corresponding to each NIRS channel as a sphere for analysis (SFA) on the basis of the photon-path-distribution function (Feng et al., 1995). For each voxel in the GM and ST layers in the SFA, we found that ~50% of the GM voxels were significantly correlated with the NIRS-Hb signals even with a strict threshold, which was corrected for the total number of object voxels (>200, see Table 2). This suggests that the photon-path-distribution function is useful and that the NIRS-Hb signals mainly reflect hemodynamics in GM. About 7–17% of the ST voxels were also significantly correlated with the NIRS-Hb signals, which indicates that the hemodynamics in the superficial layer has an effect to some extent (Firbank et al., 1998; Toronov et al., 2001). However, the correlated voxels were significantly more numerous in the GM region than in the ST region, suggesting that hemodynamic changes in GM make a dominant contribution to NIRS-Hb signals.

For a more in-depth examination of the NIRS–BOLD correlation, we derived the spatially weighted L-BOLD signal from the SFA (Sassaroli et al., 2006) as a representative temporal BOLD signal. Compared to a conventional method in which the projection point is identified on the brain surface from the midpoint between the source and detector on the scalp (Cui et al., 2011; Sasai et al., 2012), the present approach is advantageous because it takes into account the spatial dependence of the BOLD signals on the NIRS-Hb signal (Sassaroli et al., 2006). As more complex simulations using anatomical information come to be used to define voxel clusters for individual NIRS channels (Haeussinger et al., 2011; Heinzel et al., 2013), more methods for obtaining suitable BOLD signals will be developed. Nonetheless, our results and those in a previous study (Sassaroli et al., 2006) demonstrate that the present approach is useful for a quantitative comparison of NIRS and BOLD signals.

Temporal correlation of NIRS and L-BOLD signals in activation area

The results of our temporal correlation analysis between the L-BOLD (GM) and NIRS-Hb signals in the activation area showed significant correlation, a finding basically in agreement with those of previous studies (Cui et al., 2011; Heinzel et al., 2013; Mehagnoul-Schipper et al., 2002; Sassaroli et al., 2006; Strangman et al., 2002). Most previous NIRS–fMRI studies have used primary visual and/or motor tasks, which could induce a relatively reliable cortical activation, and showed a high correlation between the two modality signals. In contrast, only a few NIRS–fMRI studies have examined activation signals in the PFC. In a recent representative study (Cui et al., 2011), both the prefrontal and parietal regions were measured using a battery of cognitive tasks including finger tapping and N-back WM tasks. A comparison using the mean BOLD–NIRS correlation for all NIRS channels over a wide area of the PFC and parietal cortex revealed NIRS–BOLD correlation for both the cognitive and finger tapping tasks. However, as the strength of the correlation can be affected by whether or not the area is activated by the task, there

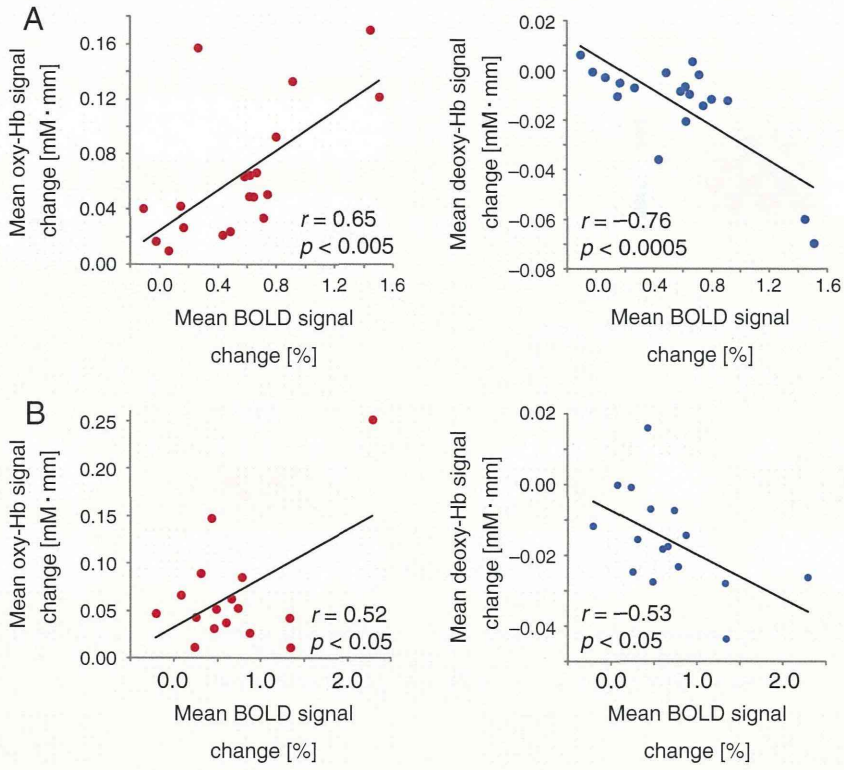

Fig. 8. Correlation between mean changes in NIRS-Hb signals and those in L-BOLD signals. Red dots indicate NIRS oxy-Hb signal and blue dots indicate NIRS deoxy-Hb signal: (A) PFC during WM task; (B) sensorimotor cortex during TAP task.

should first be a comparison of the correlation for a specified activation area known to be involved in each task. Accordingly, we compared the NIRS-Hb and L-BOLD (GM) signals for the PFC for the WM task and for the sensorimotor area for the TAP task. We found that there was correlation for both the continuous data (mean $|r|$ = 0.38–0.59, Fig. 6) and for the block-averaged data (mean $|r|$ = 0.50–0.69, Table 4) for both tasks. Our finding of correlation higher than that reported by Cui et al. (2011) (mean $|r|$ = 0.20–0.25 for each task) adds more specific information on the temporal correlation between NIRS and BOLD signals to the literature.

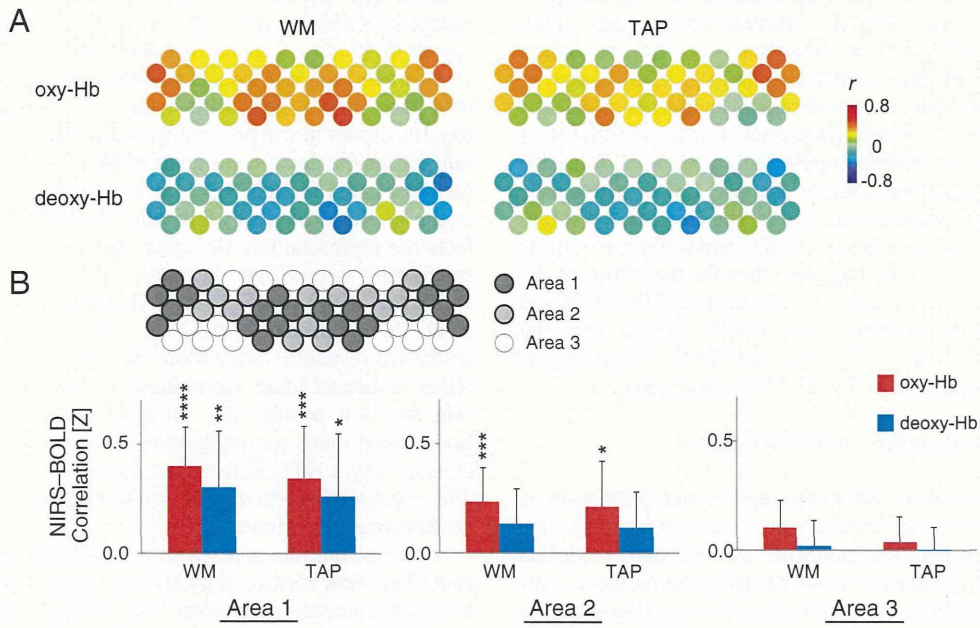

Fig. 9. Spatial distribution of correlation coefficients between NIRS-Hb and L-BOLD (GM) signals for Probe-1 data. (A) Correlation between NIRS-Hb and L-BOLD (GM) signals in WM and TAP tasks. (B) Correlation between NIRS-Hb and L-BOLD (GM) signals in three areas determined by clustering analysis using spatial pattern of correlation maps in (A). In bar graphs, mean and standard deviation of correlation coefficients (*Z*-values) between NIRS and L-BOLD signals in NIRS channels for each area are shown for WM and TAP tasks. Sign of correlation coefficients for NIRS deoxy-Hb was inverted for comparison with results for NIRS oxy-Hb signals. Statistical significance against zero is shown ($^{****}p < 10^{-5}$, $^{***}p < \times 10^{-3}$, $^{**}p < 10^{-2}$, $^{*}p < 5 \times 10^{-2}$).

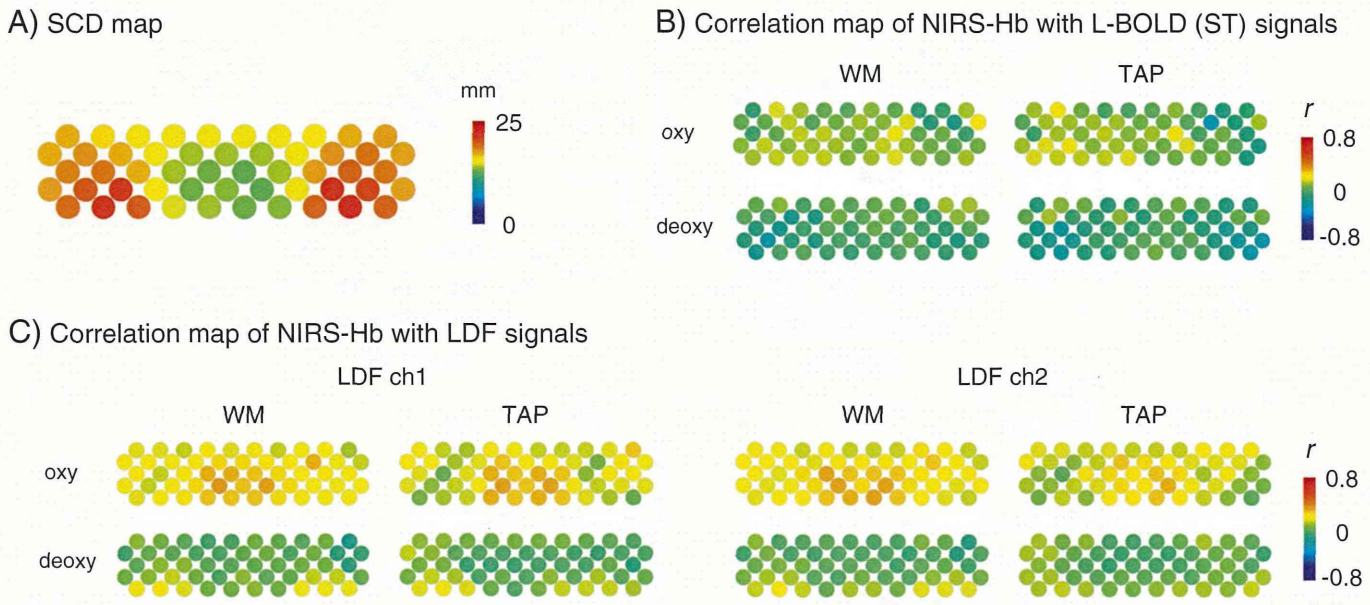

Fig. 10. Spatial distribution of potential factors affecting correlation coefficients between NIRS-Hb and BOLD signals. (A) Mean scalp-cortex distance (SCD) across 15 participants (Probe-1). Raw numerical data are shown in Supplementary Materials (Table S2). (B) Maps of correlation coefficients between NIRS-Hb and L-BOLD (ST) signals. (C) Maps of correlation coefficients between NIRS-Hb and LDF signals. LDF results for channel 1 (center point between eyebrows) are shown in the left and LDF results for channel 2 (around left temple) are shown in the right.

Amplitude correlation of NIRS and BOLD activation signals

An important finding of our study is a significant correlation between NIRS-Hb and BOLD signals in the response amplitude. This correlation was particularly evident in the PFC responses for the WM task, in which participants with a stronger NIRS-Hb response showed a stronger L-BOLD (GM) response (oxy-Hb: $r = 0.65$, deoxy-Hb: $r = -0.76$). This is the first report of amplitude correlation between NIRS-Hb and BOLD signals in the PFC, as far as we know. A similar correlation was reported for sensorimotor activation (Mehagnoul-Schipper et al., 2002). Given that the unit for the NIRS-Hb signals is the product of the change in the Hb concentration (mM) and the effective optical path length (mm), we consider that this finding demonstrates that the variation in the effective optical path length is small enough for NIRS-Hb signals to be obtained that reflect individual differences in functional activity. However, the generality of this tendency is not clear because the SCDs are variable among NIRS channels (Supplementary Material, Table S2) while the SCD in the activation area for the WM task was relatively small (13.6 ± 2.15 mm). Indeed, in the COI for the TAP task, the amplitude correlation was lower (oxy-Hb: $r = 0.52$; deoxy-Hb: $r = -0.53$) and the SCD was longer (17.6 ± 2.62 mm) than for the WM task. Although other factors such as the presence of hair should be considered for a more generalized conclusion, our results suggest that the NIRS-Hb signal amplitude for a WM task around BA46 at least reflects comparable hemodynamic information in fMRI measurements.

Effect of superficial hemodynamics on NIRS-Hb signals

We used L-BOLD signals in soft tissue regions and LDF signals as data representing extracranial hemodynamic changes to investigate the effect of superficial hemodynamics on NIRS-Hb signals. Kirilina et al. (2012) used NIRS to measure a task-related systemic signal similar to the extracranial BOLD signal of forehead veins. However, the task-related change they used was not a conventional hemodynamic response; it peaked a few seconds after task onset and linearly decreased until a few seconds after the end of the task. This change is similar to the piece-wise task-related component observed by Katura et al. (2008) and Tanaka et al. (2013). We did not observe such an uncommon pattern of NIRS-Hb signals in the activation area, probably because the conventional hemodynamic change was dominant in the proven functional areas. This pattern might be evident if a task paradigm inducing a strong systemic change is used (Kirilina et al., 2012) or if a signal-processing method that separates signal components is used (Katura et al., 2008; Tanaka et al., 2013). Although there were different sensitivities for the BOLD (GM) and BOLD (ST) signals (the intensity of the BOLD signals in GM was about 100 times that in ST, the present study nevertheless demonstrated that NIRS-Hb signals are significantly correlated with L-BOLD (GM) ones and not with L-BOLD (ST) ones. It thus provided supportive evidence that NIRS can be used to measure hemodynamic signals originating from cortical activation.

However, the LDF signals showed a time-locked increase for the WM task and a significant temporal correlation with the NIRS oxy-Hb signals in the prefrontal region. The correlation was not significant for the deoxy-Hb signals or for any of the signals in the sensorimotor area for the TAP task. This suggests that skin blood flow in the forehead increases following the WM task, which mainly affects the prefrontal oxy-Hb signals to some extent. Previous studies consistently found that the effect of systemic signals is relatively dominant in the oxy-Hb signal (Franceschini et al., 2003; Funane et al., 2013; Kirilina et al., 2012). As the amplitudes of the NIRS deoxy-Hb responses were more clearly correlated with the L-BOLD (GM) responses than were those of the NIRS oxy-Hb responses (Fig. 8A), it is possible that the NIRS deoxy-Hb signal reflected the brain signal more accurately than the oxy-Hb signal did. This might explain why a NIRS study investigating PFC activity found a robust effect supporting their conclusion only in the deoxy-Hb signal (Heilbronner and Munte, 2013).

Although additional research is needed to determine the effect of skin blood flow measured by LDF, our results demonstrated that the temporal correlation between NIRS-Hb and L-BOLD (GM) signals is significantly stronger than that between NIRS-Hb and LDF signals. Moreover, we found a correlation between the amplitudes of the NIRS-Hb and L-BOLD (GM) signals. Given these findings, we conclude that the effect of the skin blood flow is negligible in the evaluation of task-related activation, at least in BA 46, for this WM task. The

expected development of a method for separating the superficial signals from the deep brain signals will enable us to obtain NIRS-Hb signals that are less affected by skin blood flow during the performance of a wide range of tasks (Funane et al., 2013).

Spatial variability of NIRS–BOLD correlation

Correlation analysis was conducted for each NIRS channel to determine the spatial variability of the NIRS–BOLD correlations (Fig. 9). The regions in the middle of the PFC and around the sensorimotor cortices (including the inferior parietal cortex and the superior temporal cortex) showed higher correlation coefficients for both tasks. The correlation maps agree with the findings of a previous study (Cui et al., 2011), which found that the spatial pattern of the NIRS–BOLD correlations were similar across four different tasks. These results suggest that NIRS–BOLD correlation depends on the anatomical characteristics of the region as well as the task paradigm. Indeed, previous studies (Cui et al., 2011; Heinzel et al., 2013) have shown that the SCD, the GM volume penetrated by light, and the CNR contribute to the strength of the temporal correlation between the NIRS-Hb and BOLD signals. These results are reasonable given that it is natural that a larger SCD or smaller GM volume would cause lower sensitivity for cortical signals with larger noise and that a higher noise level can reduce the correlation coefficients.

Our data show that the NIRS-Hb signals in the channels in the middle of the top line and those around the bilateral temple area had almost no correlation with the BOLD signals in the GM (Fig. 9B). The larger noise level for the signals in the channels in the middle of the top line due to hair might explain their lack of correlation. The lower correlation for the NIRS-Hb signals in the channels in the temple area may have been due to an anatomical feature, such as a longer SCD (see Fig. 10A). Furthermore, the lack of correlation might be the result of a more complex phenomenon as a few previous studies have indicated that NIRS-Hb signals around the temple area are uniquely correlated with the extracranial BOLD signals (Heinzel et al., 2013; Sasai et al., 2012; Sato et al., 2011b). Although the present study did not reveal a high correlation between the L-BOLD (ST) and NIRS-Hb signals, the target frequency for the analysis might explain the difference in findings from the previous studies. The present study focused on task-related signals higher than 0.0125 Hz or 0.0150 Hz for the high-pass filtering while the previous studies focused on a lower frequency such as 0.0078 Hz (Heinzel et al., 2013), 0.0090 Hz (Sasai et al., 2012), and 0.0034 Hz (Sato et al., 2011b).

In addition, we found high temporal correlation between the LDF and NIRS oxy-Hb signals in the middle of the prefrontal region. The spatial distribution for the high correlation area was not particularly localized regardless of the LDF measurement position (Fig. 10C). This result is in agreement with those of previous studies (Aletti et al., 2012; Kohno et al., 2007) and indicates that the skin blood flow, which is measured with an LDF, affects oxy-Hb signals in a wide region of the forehead. Thus, our results indicate that there is different spatial variability between the L-BOLD (ST) and LDF signals in relation to the NIRS-Hb signals (Fig. 10). This suggests that L-BOLD (ST) signals are not sensitive to superficial skin blood flow, which can be measured with an LDF.

Limitations and future perspective

Several limitations of our study should be borne in mind. First, we took a NIRS-based approach, with our main analysis focused on the activation area determined by the NIRS-Hb signals. This approach is good for examining whether a type 1 error (false positive) occurs in the prefrontal NIRS-Hb signals but not for a type 2 error (false negative) in which NIRS fails to detect a true cortical activation. An integrated approach is needed for more precise validation of NIRS-Hb signals for functional measurements. Second, BOLD (ST) signals have a lower intensity than BOLD (GM) ones. Although previous studies have suggested the usefulness of BOLD (ST) signals for examining task-evoked extracranial signals (Heinzel et al., 2013; Kirilina et al., 2012) and our results demonstrate that NIRS-Hb signals are correlated with the BOLD (GM) signals rather than the BOLD (ST) ones, a detailed examination of the characteristics of BOLD (ST) signals is needed. Third, we examined activation signals for tasks with standard durations (~15 s), which limited us to a certain frequency band (>0.0125 Hz). We suggested that the correlation between BOLD (ST) and NIRS-Hb signals depends on the target frequency band, and the use of BOLD (ST) signals at lower frequencies (<0.01 Hz) is an issue needing to be explored. In addition, the posture of participants might be another factor influencing the effects of skin blood flow during a task. The simultaneous NIRS and fMRI measurements were performed in the supine position while normal NIRS measurements are performed in the sitting position. As a previous study reported a significant effect of head-of-bed positioning on frontal NIRS signals (Durduran et al., 2009), the effect of participant position needs to be determined.

Taking a future perspective, we see a need to clarify the factors affecting the correlation between NIRS-Hb and BOLD signals. The effect of such factors as SCD, CNR, and GM volume (Cui et al., 2011; Heinzel et al., 2013) are intertwined, making it difficult to isolate their effects by using a simple correlation analysis. There is also a need to use the simultaneous NIRS–fMRI data to validate a newly proposed method for removing the superficial hemodynamic effects (Funane et al., 2013).

Conclusion

We conducted simultaneous NIRS, fMRI, and LDF measurements to determine whether prefrontal NIRS-Hb signals reflect cortical activity rather than superficial effects. Correlation analysis demonstrated that NIRS-Hb signals in the PFC activation area are significantly correlated with BOLD signals in gray matter rather than with such signals in soft tissue or LDF signals. Moreover, the amplitudes of the task-related responses of the NIRS-Hb signals were significantly correlated with those of the L-BOLD (GM) signals across participants. These results provide supportive evidence for the validity of prefrontal NIRS-Hb signals, meaning that the NIRS-Hb signal is comparable to the BOLD signal measured by fMRI.

Acknowledgments

We thank Mr. Tsuyoshi Miyashita, Dr. Hirokazu Tanaka, and Dr. Eisuke Sakakibara for their assistance with the experiments, Dr. Daisuke Suzuki, Mr. Michiyuki Fujiwara, and Mr. Shingo Kawasaki for providing technical assistance, and Dr. Akiko Obata and Dr. Ryuta Aoki for their helpful comments on the experimental design. This study was supported by Grants-in-Aid for Scientific Research on Innovative Areas (nos. 23118001 & 23118004 [Adolescent Mind & Self-Regulation] to KK, no. 32118003 to MF, and Comprehensive Brain Science Network to KK), a Grant-in-Aid for Young Scientists (B) (no. 23791309) to RT, a Grant-in-Aid for Scientific Research (B) (no. 23390286) to MF, and a Grant-in-Aid for Challenging Exploratory Research (no. 22659209) to MF from the Ministry of Education, Culture, Sports, Science and Technology of Japan (MEXT). A part of this study was also the result of the "Development of biomarker candidates for social behavior" interdisciplinary project carried out under the Strategic Research Program for Brain Sciences by MEXT. This study was also supported in part by Health and Labor Sciences Research Grants for Comprehensive Research on Disability Health and Welfare (H23-seishin-ippan-002) to RT, YN, and MF.

Conflict of interest

Hitachi Medical Corporation provided a material support (temporary rental of a NIRS (Optical Topography) ETG-4000 system) for this study.

Appendix A. Supplementary data

Supplementary data to this article can be found online at http://dx.doi.org/10.1016/j.neuroimage.2013.06.043.

References

Aletti, F., Re, R., Pace, V., Contini, D., Molteni, E., Cerutti, S., Maria Bianchi, A., Torricelli, A., Spinelli, L., Cubeddu, R., Baselli, G., 2012. Deep and surface hemodynamic signal from functional time resolved transcranial near infrared spectroscopy compared to skin flowmotion. Comput. Biol. Med. 42, 282–289.

Aoki, R., Sato, H., Katura, T., Utsugi, K., Koizumi, H., Matsuda, R., Maki, A., 2011. Relationship of negative mood with prefrontal cortex activity during working memory tasks: an optical topography study. Neurosci. Res. 70, 189–196.

Aoki, R., Sato, H., Katura, T., Matsuda, R., Koizumi, H., 2013. Correlation between prefrontal cortex activity during working memory tasks and natural mood independent of personality effects: an optical topography study. Psychiatry Res. 212, 79–87.

Atsumori, H., Kiguchi, M., Katura, T., Funane, T., Obata, A., Sato, H., Manaka, T., Iwamoto, M., Maki, A., Koizumi, H., Kubota, K., 2010. Noninvasive imaging of prefrontal activation during attention-demanding tasks performed while walking using a wearable optical topography system. J. Biomed. Opt. 15, 046002.

Buxton, R.B., Uludag, K., Dubowitz, D.J., Liu, T.T., 2004. Modeling the hemodynamic response to brain activation. NeuroImage 23, S220–S233.

Chance, B., Zhuang, Z., UnAh, C., Alter, C., Lipton, L., 1993. Cognition-activated low-frequency modulation of light absorption in human brain. Proc. Natl. Acad. Sci. U. S. A. 90, 3770–3774.

Cohen, J., 1992. A power primer. Psychol. Bull. 112, 155–159.

Cui, X., Bray, S., Bryant, D.M., Glover, G.H., Reiss, A.L., 2011. A quantitative comparison of NIRS and fMRI across multiple cognitive tasks. NeuroImage 54, 2808–2821.

Cui, X., Bryant, D.M., Reiss, A.L., 2012. NIRS-based hyperscanning reveals increased interpersonal coherence in superior frontal cortex during cooperation. NeuroImage 59, 2430–2437.

Delpy, D.T., Cope, M., van der Zee, P., Arridge, S., Wray, S., Wyatt, J., 1988. Estimation of optical pathlength through tissue from direct time of flight measurement. Phys. Med. Biol. 33, 1433–1442.

D'Esposito, M., 2007. From cognitive to neural models of working memory. Philos. Trans. R. Soc. Lond. B Biol. Sci. 362, 761–772.

Durduran, T., Zhou, C., Edlow, B.L., Yu, G., Choe, R., Kim, M.N., Cucchiara, B.L., Putt, M.E., Shah, Q., Kasner, S.E., Greenberg, J.H., Yodh, A.G., Detre, J.A., 2009. Transcranial optical monitoring of cerebrovascular hemodynamics in acute stroke patients. Opt. Express 17, 3884–3902.

Feng, S., Zeng, F.A., Chance, B., 1995. Photon migration in the presence of a single defect: a perturbation analysis. Appl. Opt. 34, 3826–3837.

Firbank, M., Okada, E., Delpy, D.T., 1998. A theoretical study of the signal contribution of regions of the adult head to near-infrared spectroscopy studies of visual evoked responses. NeuroImage 8, 69–78.

Fisher, R.A., 1915. Frequency distribution of the values of the correlation coefficient in samples from an indefinitely large population. Biometrika 10, 507–521.

Fisher, R.A., 1921. On the "probable error" of a coefficient of correlation deduced from a small sample. Metron 1, 3–32.

Franceschini, M.A., Fantini, S., Thompson, J.H., Culver, J.P., Boas, D.A., 2003. Hemodynamic evoked response of the sensorimotor cortex measured noninvasively with near-infrared optical imaging. Psychophysiology 40, 548–560.

Funane, T., Kiguchi, M., Atsumori, H., Sato, H., Kubota, K., Koizumi, H., 2011. Synchronous activity of two people's prefrontal cortices during a cooperative task measured by simultaneous near-infrared spectroscopy. J. Biomed. Opt. 16, 077011.

Funane, T., Atsumori, H., Katura, T., Obata, A.N., Sato, H., Tanikawa, Y., Okada, E., Kiguchi, M., 2013. Quantitative evaluation of deep and shallow tissue layers' contribution to fNIRS signal using multi-distance optodes and independent component analysis. NeuroImage. http://dx.doi.org/10.1016/j.neuroimage.2013.02.026.

Genovese, C.R., Lazar, N.A., Nichols, T., 2002. Thresholding of statistical maps in functional neuroimaging using the false discovery rate. NeuroImage 15, 870–878.

Germon, T.J., Kane, N.M., Manara, A.R., Nelson, R.J., 1994. Near-infrared spectroscopy in adults: effects of extracranial ischaemia and intracranial hypoxia on estimation of cerebral oxygenation. Br. J. Anaesth. 73, 503–506.

Germon, T.J., Evans, P.D., Manara, A.R., Barnett, N.J., Wall, P., Nelson, R.J., 1998. Sensitivity of near infrared spectroscopy to cerebral and extra-cerebral oxygenation changes is determined by emitter-detector separation. J. Clin. Monit. Comput. 14, 353–360.

Goldman-Rakic, P.S., 1987. Circuitry of primate prefrontal cortex and regulation of behavior by representational memory. In: Plum, F. (Ed.), Handbook of Physiology. The Nervous System. Higher Functions of the Brain. American Physiological Society, Bethesda, MD.

Haeussinger, F.B., Heinzel, S., Hahn, T., Schecklmann, M., Ehlis, A.C., Fallgatter, A.J., 2011. Simulation of near-infrared light absorption considering individual head and prefrontal cortex anatomy: implications for optical neuroimaging. PLoS One 6, e26377.

Heilbronner, U., Munte, T.F., 2013. Rapid event-related near-infrared spectroscopy detects age-related qualitative changes in the neural correlates of response inhibition. NeuroImage 65, 408–415.

Heinzel, S., Haeussinger, F.B., Hahn, T., Ehlis, A.C., Plichta, M.M., Fallgatter, A.J., 2013. Variability of (functional) hemodynamics as measured with simultaneous fNIRS and fMRI during intertemporal choice. NeuroImage 71, 125–134.

Homae, F., Watanabe, H., Otobe, T., Nakano, T., Go, T., Konishi, Y., Taga, G., 2010. Development of global cortical networks in early infancy. J. Neurosci. 30, 4877–4882.

Hoshi, Y., Tamura, M., 1993. Detection of dynamic changes in cerebral oxygenation coupled to neuronal function during mental work in man. Neurosci. Lett. 150, 5–8.

Huppert, T.J., Hoge, R.D., Diamond, S.G., Franceschini, M.A., Boas, D.A., 2006. A temporal comparison of BOLD, ASL, and NIRS hemodynamic responses to motor stimuli in adult humans. NeuroImage 29, 368–382.

Jöbsis, F.F., 1977. Noninvasive, infrared monitoring of cerebral and myocardial oxygen sufficiency and circulatory parameters. Science 198, 1264–1267.

Jöbsis-VanderVliet, F.F., Piantadosi, C.A., Sylvia, A.L., Lucas, S.K., Keizer, H.H., 1988. Near-infrared monitoring of cerebral oxygen sufficiency. I. Spectra of cytochrome c oxidase. Neurol. Res. 10, 7–17.

Kato, T., Kamei, A., Takashima, S., Ozaki, T., 1993. Human visual cortical function during photic stimulation monitoring by means of near-infrared spectroscopy. J. Cereb. Blood Flow Metab. 13, 516–520.

Katura, T., Sato, H., Fuchino, Y., Yoshida, T., Atsumori, H., Kiguchi, M., Maki, A., Abe, M., Tanaka, N., 2008. Extracting task-related activation components from optical topography measurement using independent components analysis. J. Biomed. Opt. 13, 054008.

Kirilina, E., Jelzow, A., Heine, A., Niessing, M., Wabnitz, H., Bruhl, R., Ittermann, B., Jacobs, A.M., Tachtsidis, I., 2012. The physiological origin of task-evoked systemic artefacts in functional near infrared spectroscopy. NeuroImage 61, 70–81.

Kleinschmidt, A., Obrig, H., Requardt, M., Merboldt, K.D., Dirnagl, U., Villringer, A., Frahm, J., 1996. Simultaneous recording of cerebral blood oxygenation changes during human brain activation by magnetic resonance imaging and near-infrared spectroscopy. J. Cereb. Blood Flow Metab. 16, 817–826.

Kohno, S., Miyai, I., Seiyama, A., Oda, I., Ishikawa, A., Tsuneishi, S., Amita, T., Shimizu, K., 2007. Removal of the skin blood flow artifact in functional near-infrared spectroscopic imaging data through independent component analysis. J. Biomed. Opt. 12, 062111.

Kubota, K., Niki, H., 1971. Prefrontal cortical unit activity and delayed alternation performance in monkeys. J. Neurophysiol. 34, 337–347.

Maki, A., Yamashita, Y., Ito, Y., Watanabe, E., Mayanagi, Y., Koizumi, H., 1995. Spatial and temporal analysis of human motor activity using noninvasive NIR topography. Med. Phys. 22, 1997–2005.

McCarthy, G., Blamire, A.M., Puce, A., Nobre, A.C., Bloch, G., Hyder, F., Goldman-Rakic, P., Shulman, R.G., 1994. Functional magnetic resonance imaging of human prefrontal cortex activation during a spatial working memory task. Proc. Natl. Acad. Sci. U. S. A. 91, 8690–8694.

McCarthy, G., Puce, A., Constable, R.T., Krystal, J.H., Gore, J.C., Goldman-Rakic, P., 1996. Activation of human prefrontal cortex during spatial and nonspatial working memory tasks measured by functional MRI. Cereb. Cortex 6, 600–611.

Mehagnoul-Schipper, D.J., van der Kallen, B.F., Colier, W.N., van der Sluijs, M.C., van Erning, L.J., Thijssen, H.O., Oeseburg, B., Hoefnagels, W.H., Jansen, R.W., 2002. Simultaneous measurements of cerebral oxygenation changes during brain activation by near-infrared spectroscopy and functional magnetic resonance imaging in healthy young and elderly subjects. Hum. Brain Mapp. 16, 14–23.

Millikan, G.A., 1942. The oxymeter, an instrument for measuring continuously the oxygen saturation of arterial blood in man. Rev. Sci. Instrum. 13, 434–444.

Minagawa-Kawai, Y., van der Lely, H., Ramus, F., Sato, Y., Mazuka, R., Dupoux, E., 2011. Optical brain imaging reveals general auditory and language-specific processing in early infant development. Cereb. Cortex 21, 254–261.

Miyai, I., Tanabe, H.C., Sase, I., Eda, H., Oda, I., Konishi, I., Tsunazawa, Y., Suzuki, T., Yanagida, T., Kubota, K., 2001. Cortical mapping of gait in humans: a near-infrared spectroscopic topography study. NeuroImage 14, 1186–1192.

Ogawa, S., Lee, T.M., Kay, A.R., Tank, D.W., 1990a. Brain magnetic resonance imaging with contrast dependent on blood oxygenation. Proc. Natl. Acad. Sci. U. S. A. 87, 9868–9872.

Ogawa, S., Lee, T.M., Nayak, A.S., Glynn, P., 1990b. Oxygenation-sensitive contrast in magnetic resonance image of rodent brain at high magnetic fields. Magn. Reson. Med. 14, 68–78.

Pena, M., Maki, A., Kovacic, D., Dehaene-Lambertz, G., Koizumi, H., Bouquet, F., Mehler, J., 2003. Sounds and silence: an optical topography study of language recognition at birth. Proc. Natl. Acad. Sci. U. S. A. 100, 11702–11705.

Rorden, C., Brett, M., 2000. Stereotaxic display of brain lesions. Behav. Neurol. 12, 191–200.

Sasai, S., Homae, F., Watanabe, H., Sasaki, A.T., Tanabe, H.C., Sadato, N., Taga, G., 2012. A NIRS–fMRI study of resting state network. NeuroImage 63, 179–193.

Sassaroli, A., de, B.F.B., Tong, Y., Renshaw, P.F., Fantini, S., 2006. Spatially weighted BOLD signal for comparison of functional magnetic resonance imaging and near-infrared imaging of the brain. NeuroImage 33, 505–514.

Sato, H., Fuchino, Y., Kiguchi, M., Katura, T., Maki, A., Yoro, T., Koizumi, H., 2005. Intersubject variability of near-infrared spectroscopy signals during sensorimotor cortex activation. J. Biomed. Opt. 10, 044001.

Sato, H., Kiguchi, M., Maki, A., Fuchino, Y., Obata, A., Yoro, T., Koizumi, H., 2006. Within-subject reproducibility of near-infrared spectroscopy signals in sensorimotor activation after 6 months. J. Biomed. Opt. 11, 014021.

Sato, H., Aoki, R., Katura, T., Matsuda, R., Koizumi, H., 2011a. Correlation of within-individual fluctuation of depressed mood with prefrontal cortex activity during verbal working memory task: optical topography study. J. Biomed. Opt. 16, 126007.

Sato, H., Obata, A.N., Moda, I., Ozaki, K., Yasuhara, T., Yamamoto, Y., Kiguchi, M., Maki, A., Kubota, K., Koizumi, H., 2011b. Application of near-infrared spectroscopy to measurement of hemodynamic signals accompanying stimulated saliva secretion. J. Biomed. Opt. 16, 047002.

Sato, H., Hirabayashi, Y., Tsubokura, H., Kanai, M., Ashida, T., Konishi, I., Uchida-Ota, M., Konishi, Y., Maki, A., 2012. Cerebral hemodynamics in newborn infants exposed to speech sounds: a whole-head optical topography study. Hum. Brain Mapp. 33, 2092–2103.

Strangman, G., Culver, J.P., Thompson, J.H., Boas, D.A., 2002. A quantitative comparison of simultaneous BOLD fMRI and NIRS recordings during functional brain activation. NeuroImage 17, 719–731.

Taga, G., Asakawa, K., Maki, A., Konishi, Y., Koizumi, H., 2003. Brain imaging in awake infants by near-infrared optical topography. Proc. Natl. Acad. Sci. U. S. A. 100, 10722–10727.

Takahashi, T., Takikawa, Y., Kawagoe, R., Shibuya, S., Iwano, T., Kitazawa, S., 2011. Influence of skin blood flow on near-infrared spectroscopy signals measured on the forehead during a verbal fluency task. NeuroImage 57, 991–1002.

Tanaka, H., Katura, T., Sato, H., 2013. Task-related component analysis for functional neuroimaging and application to near-infrared spectroscopy data. NeuroImage 64, 308–327.

Toronov, V., Webb, A., Choi, J.H., Wolf, M., Michalos, A., Gratton, E., Hueber, D., 2001. Investigation of human brain hemodynamics by simultaneous near-infrared spectroscopy and functional magnetic resonance imaging. Med. Phys. 28, 521–527.

Toronov, V., Walker, S., Gupta, R., Choi, J.H., Gratton, E., Hueber, D., Webb, A., 2003. The roles of changes in deoxyhemoglobin concentration and regional cerebral blood volume in the fMRI BOLD signal. NeuroImage 19, 1521–1531.

Tsujimoto, S., Postle, B.R., 2012. The prefrontal cortex and oculomotor delayed response: a reconsideration of the "mnemonic scotoma". J. Cogn. Neurosci. 24, 627–635.

Tsujimoto, S., Yamamoto, T., Kawaguchi, H., Koizumi, H., Sawaguchi, T., 2004. Prefrontal cortical activation associated with working memory in adults and preschool children: an event-related optical topography study. Cereb. Cortex 14, 703–712.

Villringer, A., Planck, J., Hock, C., Schleinkofer, L., Dirnagl, U., 1993. Near infrared spectroscopy (NIRS): a new tool to study hemodynamic changes during activation of brain function in human adults. Neurosci. Lett. 154, 101–104.

Wray, S., Cope, M., Delpy, D.T., Wyatt, J.S., 1988. Characterization of the near infrared absorption spectra of cytochrome aa3 and haemoglobin for the non-invasive monitoring of cerebral oxygenation. Biochim. Biophys. Acta 933, 184–192.

Yamashita, Y., Maki, A., Ito, Y., Watanabe, E., Mayanagi, H., Koizumi, H., 1996. Noninvasive near-infrared topography of human brain activity using intensity modulation spectroscopy. Opt. Eng. 35, 1046–1049.

Journal of Psychiatric Research 47 (2013) 1581–1589

Contents lists available at ScienceDirect

Journal of Psychiatric Research

journal homepage: www.elsevier.com/locate/psychires

Temporal lobe and inferior frontal gyrus dysfunction in patients with schizophrenia during face-to-face conversation: A near-infrared spectroscopy study

Yuichi Takei*, Masashi Suda, Yoshiyuki Aoyama, Miho Yamaguchi, Noriko Sakurai, Kosuke Narita, Masato Fukuda, Masahiko Mikuni

Department of Psychiatry and Neuroscience, Gunma University of Graduate School of Medicine, 3-39-22 Showa, Maebashi, Gunma 371-8511, Japan

ARTICLE INFO

Article history:
Received 18 September 2012
Received in revised form
26 July 2013
Accepted 31 July 2013

Keywords:
Near-infrared spectroscopy
Positive and Negative Syndrome Scale
Schizophrenia
Social cognition
Talk
Face-to-face conversation

ABSTRACT

Schizophrenia (SC) is marked by poor social-role performance and social-skill deficits that are well reflected in daily conversation. Although the mechanism underlying these impairments has been investigated by functional neuroimaging, technical limitations have prevented the investigation of brain activation during conversation in typical clinical situations. To fill this research gap, this study investigated and compared frontal and temporal lobe activation in patients with SC during face-to-face conversation. Frontal and temporal lobe activation in 29 patients and 31 normal controls (NC) ($n = 60$) were measured during 180-s conversation periods by using near-infrared spectroscopy (NIRS). The grand average values of oxyhemoglobin concentration ([oxy-Hb]) changes during task performance were analyzed to determine their correlation with clinical variables and Positive and Negative Syndrome Scale (PANSS) subscores. Compared to NCs, patients with SC exhibited decreased performance in the conversation task and decreased activation in both the temporal lobes and the right inferior frontal gyrus (IFG) during task performance, as indicated by the grand average of [oxy-Hb] changes. The decreased activation in the left temporal lobe was negatively correlated with the PANSS disorganization and negative symptoms subscores and that in the right IFG was negatively correlated with illness duration, PANSS disorganization, and negative symptom subscores. These findings indicate that brain dysfunction in SC during conversation is related to functional deficits in both the temporal lobes and the right IFG and manifests primarily in the form of disorganized thinking and negative symptomatology.

1. Introduction

Schizophrenia (SC) is marked by poor social performance, which is a complex phenomenon influenced by many affective, motivational, and environmental factors. Deficiency in *social skills*, a behavioral construct reflecting the smooth application of several specific verbal and nonverbal abilities and cognitive capacities involved in daily conversation, is a critical component of SC. Typically, clinicians diagnose SC on the basis of behavioral observation and analysis of speech content, attitude, and emotional response during interviews. Neuropsychological testing and functional neuroimaging have confirmed that patients with SC have basic cognitive deficits, such as deficits in working and verbal memory and attention (Mohamed et al., 1999; Riley et al., 2000), which are related to impairment in various brain regions, primarily the frontal and temporal lobes, and contribute to their social-skill deficits.

Social cognition is one of the crucial factors necessary for having a conversation. The mainstream of social cognition studies is mental-state attribution, i.e., "theory of mind" (ToM) or "mentalizing," which involves the ability to assume the intentions, beliefs, wishes, feelings, and knowledge states of other individuals based on either observational input ("mental-state decoding") or inferential processes ("mental-state reasoning") (Brune and Schaub, 2012). Many recent studies have reported that the reduced volume and/or reduced activation of gray matter in specific brain regions, mainly the temporal lobe, ventromedial prefrontal cortex (PFC), and cingulate cortex, are associated with the ToM deficits shown by patients with SC (Benedetti et al., 2009; Hooker et al., 2011; Sugranyes et al., 2011). Although the mechanism underlying this phenomenon has been investigated by functional neuroimaging, technical limitations have prevented the investigation of brain activation during conversation in typical clinical situations.

* Corresponding author. Tel./fax: +81 27 220 8183.
E-mail address: tyuichi@gunma-u.ac.jp (Y. Takei).

0022-3956/$ – see front matter © 2013 Elsevier Ltd. All rights reserved.
http://dx.doi.org/10.1016/j.jpsychires.2013.07.029

Therefore, the manner of brain functioning and the consequent integration of various cognitive functions during conversation remain unclear.

Near-infrared spectroscopy (NIRS) has the advantage that brain activation can be evaluated in a naturalistic environment. Several recent studies reported use of NIRS during face-to-face interaction (Costantini et al., 2013; Cui et al., 2012; Konvalinka and Roepstorff, 2012). However, few studies have investigated its application during face-to-face conversation (Suda et al., 2010, 2011).

In this study, we used NIRS to investigate frontal and temporal lobe activation in patients with SC during conversation. Because SC characteristics are well reflected in conversation, we hypothesized that (i) patients with SC and NCs exhibit differences in frontal and temporal lobe activation during conversation, (ii) patients with SC and NCs exhibit differences in behavior during conversation, and (iii) alterations in frontal and temporal lobe activations correlate with clinical symptoms and/or behavior.

2. Materials and methods

2.1. Participants

We recruited 29 patients with SC and 31 NCs ($n = 60$) from the Department of Psychiatry and Neuroscience, Gunma University Hospital, Japan (Table 1). SC diagnosis was based on the Diagnostic and Statistical Manual of Mental Disorders, Fourth Edition (DSM-IV) criteria. Patients older than 60 were not included, to eliminate the possible interference of additional pathophysiological factors, such as aging and cerebrovascular changes. All patients were taking medications, including antipsychotics, mood stabilizers, antidepressants, anxiolytics, hypnotics, and/or antiparkinsonian drugs. The chlorpromazine equivalent dose of antipsychotics, imipramine equivalent dose of antidepressants, diazepam equivalent dose of anxiolytics, and flunitrazepam equivalent dose of hypnotics were calculated for each patient (Inagaki, 2006). All patients were clinically stable, as indicated by their scores on the Positive and Negative Syndrome Scale (PANSS), which assesses the 5 psychiatric factors of positive symptomatology, negative symptomatology, disorganization, excitement, and emotional distress (Kay et al., 1987; van der Gaag et al., 2006). NCs had no history of major psychiatric or physical illness or took any medications. All subjects were right-handed and native Japanese speakers. The exclusion criteria for both groups included clear abnormality in brain magnetic resonance imaging (MRI) results, neurological illness, traumatic brain injury with any of the known cognitive consequences or loss of consciousness for more than 5 min, substance use or addiction, and presence of hearing or vision impairment. This study was performed in accordance with the Helsinki Declaration, as revised in 1989, and was approved by the Institutional Review Board of the Gunma University Hospital. Written informed consent was obtained from all subjects before study initiation. If a patient was younger than 20 years or had been forcibly committed to hospitalization, written informed consent was obtained from his/her legal representative. Because we could not obtain behavioral data of conversations from subjects who had not provided consent for videotape recording, we describe the clinical characteristics of all subjects using the behavioral data listed in Table 1.

2.2. Activation tasks

Two types of activation tasks, a conversation and a control task, were used to assess brain activation during conversation (Fig. 1).

Table 1
Subject characteristics. The data presented on the left side (groups of total subjects) indicate the characteristics of the subjects who participated in this study, whereas the data presented on the right side (subgroups of subjects with behavioral data) indicate the characteristics of the subgroup of subjects with behavioral data. Antipsychotics, chlorpromazine equivalent dose; antidepressants, imipramine equivalent dose; anxiolytics, diazepam equivalent dose; and hypnotics, flunitrazepam equivalent dose. M, male; F, female; SC, schizophrenic subjects; NC, normal controls; ST, speaking time score; RS, receiving aspect score; SS, sending aspect score; GAF, Global Assessment of Functioning; PANSS, Positive and Negative Symptom Scale.

	Groups of total subjects				Subgroups of subjects with behavioral data			
	SC ($n = 29$)		NC ($n = 31$)		SC ($n = 15$)		NC ($n = 28$)	
	M	F	M	F	M	F	M	F
Sex	19	10	20	11	9	6	18	11
	Mean	SD	Mean	SD	Mean	SD	Mean	SD
Age (year)	35.4	11.9	33.5	10	34.3	12.1	32.6	9.7
Age range (year)	19–58		23–58		19–57		23–58	
Age of onset (year)	23.6	7.3			24.3	8.4		
Illness duration (year)	11.6	8.8			10.2	7.9		
GAF					55.8	13.0		
PANSS five-factor model	Mean	SD			Mean	SD		
Positive symptoms	11.6	4.1			10.3	3.3		
Negative symptoms	21.4	8.4			19.8	5.9		
Disorganization	10	4.2			8.1	1.7		
Excitement	6.6	3.1			5.3	1.5		
Emotional distress	8.5	2.7			8.0	2.6		
Medications	Mean	SD	*n*		Mean	SD	*n*	
Antipsychotic (mg/day)	621.9	574.1	26/29		471.8	435.5	14/15	
Antipsychotic (mg/day)	51.8	65.7	4/29		60.7	77.5	3/15	
Anxiolytic (mg/day)	7.4	6.3	10/29		6.0	6.2	5/15	
Hypnotic (mg/day)	1.9	1.1	10/29		1.8	1.0	4/15	
Behavioral data					Mean	SD	Mean	SD
Time (s)					70.3	9.9	77.7	4.9
RS					3.0	0.9	4.0	0.2
SS					2.6	1.0	3.4	0.9